

Magnetic anisotropy in ferromagnetic Josephson junctions

M. Weides

Citation: [Appl. Phys. Lett.](#) **93**, 052502 (2008);

View online: <https://doi.org/10.1063/1.2967873>

View Table of Contents: <http://aip.scitation.org/toc/apl/93/5>

Published by the [American Institute of Physics](#)

Articles you may be interested in

[Switching at small magnetic fields in Josephson junctions fabricated with ferromagnetic barrier layers](#)

Applied Physics Letters **104**, 022602 (2014); 10.1063/1.4862195

[Spin-transfer switching of orthogonal spin-valve devices at cryogenic temperatures](#)

Journal of Applied Physics **115**, 17C725 (2014); 10.1063/1.4865464

[Spin-polarized supercurrents for spintronics](#)

Physics Today **64**, 43 (2011); 10.1063/1.3541944

[Controllable Josephson current through a pseudospin-valve structure](#)

Applied Physics Letters **84**, 1153 (2004); 10.1063/1.1646217

[High quality ferromagnetic 0 and \$\pi\$ Josephson tunnel junctions](#)

Applied Physics Letters **89**, 122511 (2006); 10.1063/1.2356104



Scilight

Sharp, quick summaries **illuminating**
the latest physics research

Sign up for **FREE!**

AIP
Publishing

Magnetic anisotropy in ferromagnetic Josephson junctions

M. Weides

Center of Nanoelectronic Systems for Information Technology and Institute of Solid State Research,
Research Centre Jülich, D-52425 Jülich, Germany

(Received 26 May 2008; accepted 13 July 2008; published online 5 August 2008)

Magnetotransport measurements were done on Nb/Al₂O₃/Cu/Ni/Nb superconductor-insulator-ferromagnet-superconductor Josephson tunnel junctions. Depending on ferromagnetic Ni interlayer thickness and geometry, the standard (1d) magnetic field dependence of critical current deviates from the textbook model for Josephson junctions. The results are qualitatively explained by a short Josephson junction model based on anisotropy and 2d remanent magnetization. © 2008 American Institute of Physics. [DOI: 10.1063/1.2967873]

Superconductivity (S) and ferromagnetism (F) in thin layered films have now been studied during some decades.¹ In SF bilayers the superconductivity may be nonuniform, i.e., the Cooper pair wave function extends to the ferromagnet with an oscillatory behavior. In Josephson junctions (JJs) based on *s*-wave superconductors the phase coupling between the superconducting electrodes can be shifted by π when using a ferromagnetic barrier with an appropriate chosen thickness d_F , i.e., SFS or SIFS-type junctions (I: insulating tunnel barrier). Only in recent years the experimental realization of π JJs was successful. In particular, the π coupling was demonstrated by varying the temperature,²⁻⁴ the thickness of the F-layer,^{4,7} or measuring the current-phase relation of JJs incorporated into a superconducting loop.⁸⁻¹⁰ The coupling can also change within a single JJ by a steplike F-layer, i.e., one-half is a 0 JJ and the other half is a π JJ.^{11,12}

For useful classical or quantum circuits based on SFS/SIFS JJs, a large critical current density j_c (small Josephson penetration depth λ_J) and a high $I_c R$ product are needed.^{13,14} Up to now the limiting factor is the low j_c due to a strong Cooper pair breaking inside F-layer. Alloys of magnetic and nonmagnetic atoms such as NiCu face problems of clustering¹⁵ and magnetic scattering.^{4,7} Promising experiments using strong magnets^{5,16-19} were published.

Shape anisotropy of magnetic interlayer may provoke a not flux-closed domain structure and consequently a shift of critical current diffraction pattern $I_c(H)$.¹⁸ In experiments,^{2,4,6,18,19} the SFS/SIFS JJs had nearly mirror symmetrical $I_c(H)$, i.e., the effective shift along the H -axis is small, usually less than one flux quantum Φ_0 . This is explained by a multidomain state of F-layer with a very small net magnetization. However, up to now the 2d nature of thin-film magnetism was disregarded.

In this letter the $I_c(H)$ dependence for remanent 2d magnetization of F-layer is systematically studied. First, the maximal flux from F-layer is estimated. Second, the $I_c(H)$ pattern considering 2d in-plane magnetization is calculated for different aspect ratios. Third, the $I_c(H)$ pattern is measured along both magnetic axes for various junction geometries and d_F .

The maximal shift of $I_c(H_y)$ is estimated for a strong magnet, i.e., Ni, being magnetized fully in plane and along the y -axis. The atomic magnetic momentum is $0.6\mu_B$,²⁰ the specific density ρ is 8.9 g/cm^3 (bulk), and magnetization $\mu_0 M = 0.64 \text{ T}$. A cross section of length $L_x = 100 \mu\text{m}$ and F-layer thickness $d_F = 3 \text{ nm}$ encloses a magnetic flux Φ_M

$= d_F L_x \mu_0 M$. The total magnetic flux Φ through the JJ is the applied field flux $\Phi_H = (2\lambda_L + d_F)L_x H_y$ (London penetration depth $\lambda_L = 90 \text{ nm}$) plus Φ_M , i.e., $\Phi = \Phi_H \pm \Phi_M = 8.85\Phi_0 H_y / \text{mT} \pm 92\Phi_0$. The $I_c(H_y)$ pattern is shifted by 92 periods from the center. This simple calculation neglects dead magnetic layer,²¹ as found in SFS/SIFS JJs,^{4,7,19} and demagnetizing by domains. Real Ni films tend to form complex magnetization profiles (in/out of plane) and domain structures as function of d_F .²² Integral magnetization measurements in SF layers show a complex behavior as a function of temperature, applied field, and sample history,^{23,24} e.g., SF structures spontaneously alter their stray field by changing magnetic domain distribution.²⁵ The local magnetization depends on stray fields from neighbor domains, flux focusing from S-electrodes,^{18,26} or on bias induced spin accumulation at F/S interface.²⁷ It is generally agreed that the average magnetization in SFS/SIFS JJs is much smaller than the maximum magnetization estimated above. However, as shown below even a remanent 2d magnetization of 1% of the maximal value may notably change the $I_c(H)$ pattern.

A qualitative model for $I_c(H)$ in presence of a uniform fixed 2d magnetization \vec{M} is derived. The short JJ model

$$I_c(H) = I_c^0 \left| \frac{\sin\left(\frac{\pi \Phi}{\Phi_0}\right)}{\frac{\Phi}{\pi \Phi_0}} \right| \quad \text{and } \Phi = \Phi_H \pm \Phi_M$$

is modified by 2d distributions of applied field flux Φ_H and magnetization Φ_M with

$$\Phi = \left[\begin{pmatrix} 0 & H_x \\ H_y & 0 \end{pmatrix} \pm \begin{pmatrix} \alpha & 0 \\ 0 & \alpha \end{pmatrix} \right] \times \begin{pmatrix} L_x \\ L_y \end{pmatrix}.$$

$\vec{M} = \alpha(L_x, L_y)$ is assumed to be orientated in-plane (Meissner-screening of S-electrodes) along the diagonal (i.e., longest) axis of sample (rough approximation for magnetic shape anisotropy). The magnetization \vec{M} is several orders of magnitude smaller than the upper limit given by a fully saturated magnetic layer. Note that the easy axis of ferromagnetic film can be determined by the magnetic field during deposition, too. The model for Φ_M is just exemplary for the effect of 2d in-plane magnetization in $I_c(H)$.

In Fig. 1, the surface plot of $I_c(H_x, H_y)$ is depicted for various α and geometries. The position of I_c^0 is shifted from the center ($H_x = H_y = 0 \text{ mT}$) in opposite direction of \vec{M} . Figure

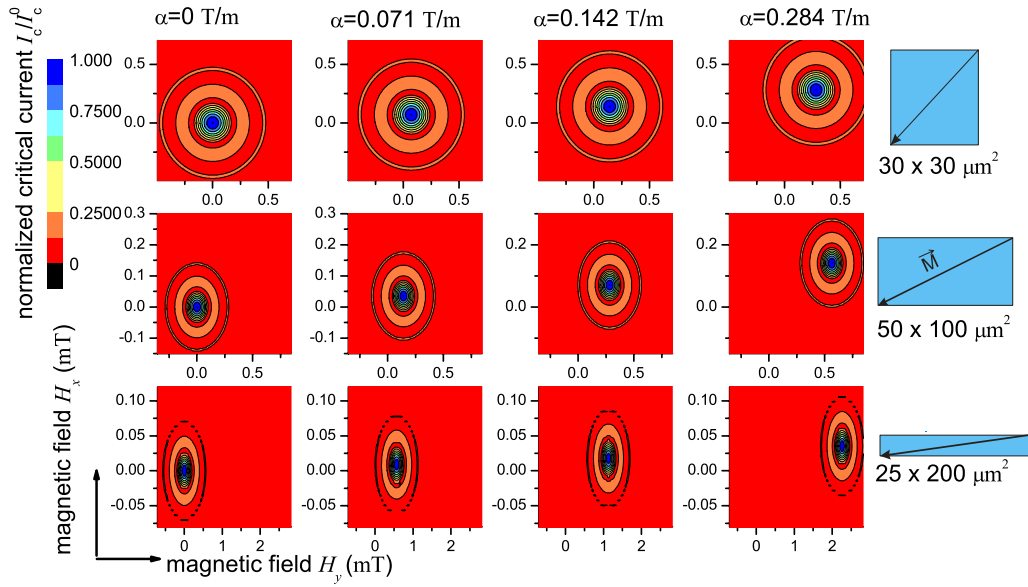


FIG. 1. (Color online) Calculated surface plot of $I_c(H_x, H_y)$ for different geometries and remanent magnetizations α . The magnetization vector \vec{M} points from top right to bottom left corner (arrow) and I_c^0 is shifted in opposite direction.

2 depicts $I_c(H_x, 0)$ and $I_c(0, H_y)$ patterns. These graphs resemble standard 1d $I_c(H)$ ($H=H_x, H_y$) measurements. For some $|\vec{M}| \neq 0$ T, a single-peaked $I_c(H_x)$, $I_c(H_y)$ pattern is calculated, which—on first glance—resembles a shifted $|\sin(H)/H|$ Fraunhofer pattern. However, the maximum I_c is smaller than the real I_c^0 and the height of side maxima does not obey the expected value. For example, the $I_c(H_x, 0)$ pattern of $30 \times 30 \mu\text{m}^2$ sample and $\alpha=0.071$ T/m is shifted by less than Φ_0 and its maximum I_c is already reduced to $\sim 0.8I_c^0$. This simple $I_c(H_x, H_y)$ model may qualitatively explain some experimental observations (Fig. 3) on SIFS-type JJs with Ni interlayer.

For experiment JJs with similar areas, i.e., 30×30 , 50×100 , and $25 \times 200 \mu\text{m}^2$, were fabricated. The SIFS multilayer was sputter deposited with d_F ranging from 1 to 6 nm. The tunnel barrier was formed for 30 min at a partial oxygen pressure of 0.1 mbar. After oxidation a 2 nm

Cu film was inserted. All JJs were deposited in a single run by shifting the substrate and target to obtain a wedge-shaped Ni layer.²⁸ Normal state and subgap resistance indicate a small junction to junction variation. The IV and $I_c(H_x)$, $I_c(H_y)$ characteristics were measured at 4.2 K for two sets of samples ($d_F=2.2$ and 3.9 nm). Cooldown was done in zero field and thermal cycling up to ≈ 15 and 300 K to check reproducibility. Measurements were made in a liquid He dip probe using low-noise homemade electronics and room-temperature voltage amplifier. The fields ($H_x, 0$), ($0, H_y$) were applied in plane of the sample and parallel the junctions axis (Fig. 1). The voltage criteria V_c for $I_c(H)$ determination were $0.2\text{--}1 \mu\text{V}$. A lower subgap resistance for $d_F=3.9$ nm sample leads to larger offset currents. Positive and negative current branches of IVC had similar magnetic field dependence $+I_c(H_y) \approx |-I_c(H_y)|$. Magnetic field was swept between ± 1.5 mT for all samples. All junctions had their lateral sizes

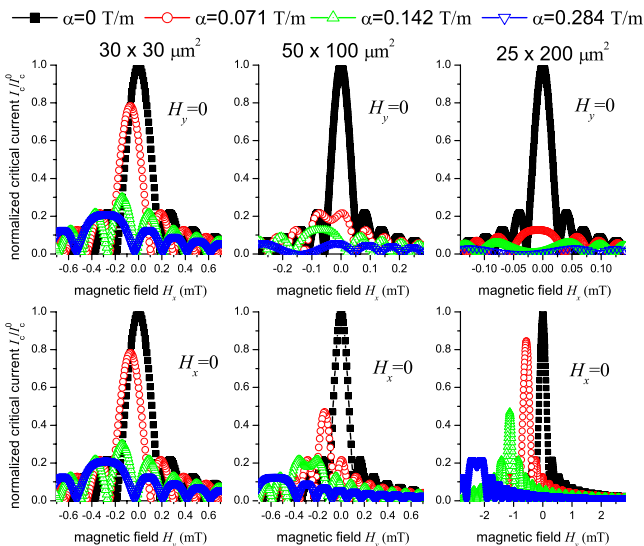


FIG. 2. (Color online) Calculated I_c as function of 1d magnetic field, $I_c(H_x, 0)$ (top), and $I_c(0, H_y)$ (bottom) for the three geometries and various α . A substantial deviation from ideal ($\alpha=0$ T/m) pattern appears for already small magnetization vector $\vec{M}=\alpha(L_x, L_y)$.

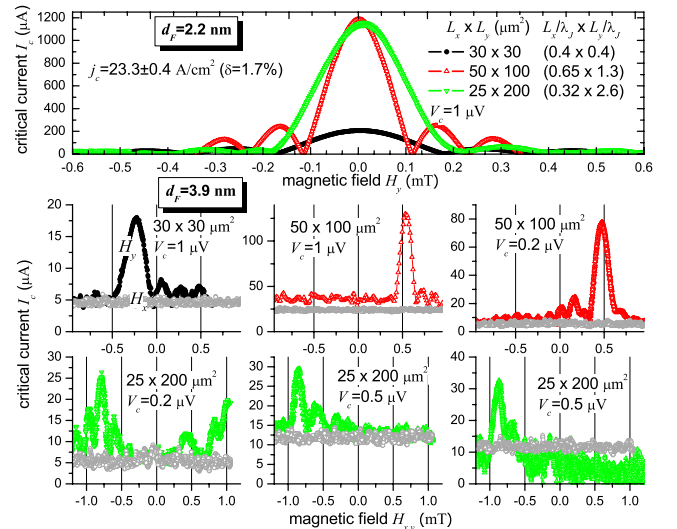


FIG. 3. (Color online) Measured $I_c(H_y)$ pattern of SIFS JJs for thin (top) and thick (bottom) Ni layers and different geometries. $I_c(H_x)$ pattern of thick Ni layer is plotted in gray. Onset of magnetic anisotropy effects in Ni layer is between 2.2 and 3.9 nm.

comparable or smaller than the Josephson penetration length λ_J , except the longest sample ($d_F=2.2$ nm, $25 \times 200 \mu\text{m}^2$), whose L_y is not strictly inside the short JJ limit.

The $d_F=2.2$ nm samples showed very regular $I_c(H_y)$ pattern. All maximum I_c 's were nearly centered and the spread of j_c was $\sim 1.7\%$, as determined from the maximum I_c 's. The $I_c(H_x)$ pattern is symmetric, too (not shown). The oscillation period of $I_c(H_y)$ was determined by magnetic cross section $\sim 1/L_x$, and nearly independent of aspect ratio. No indication for a distorted supercurrent transport due to alloying at the Nb/Ni interface²⁹ can be found. Effects due to magnetic anisotropy were not detectable, either because the samples were still inside the dead magnetic layer or the anisotropy was absent or totally out of plane.

The $d_F=3.9$ nm samples had completely different $I_c(H_y)$ pattern showing in-plane anisotropy with some characteristic features. All maximum I_c 's were shifted from the center, and the amplitude of shift increased with L_y , i.e., ≈ 0.24 mT for $30 \times 30 \mu\text{m}^2$, ≈ 0.5 mT for $50 \times 100 \mu\text{m}^2$, and ≈ 0.8 mT for $25 \times 200 \mu\text{m}^2$ samples. The direction of shift varies between samples even if they were cooled and measured at the same time (random polarity of magnetic configuration). The position of main peak of $I_c(H_y)$ was reproducible after thermal cycling to 300 K. The width of main maxima (measured at offset line) was not strictly $\sim 1/L_x$, and varies from sample to sample. The pattern were asymmetric, i.e., the height of same-order side maxima differed, probably due to nonuniform flux guidance in F-layer and reorientation of domains.

By rotating the magnetic field by 90° , i.e., measuring in $I_c(H_x)$ mode, low I_c 's, being nearly independent of H_x , were detected. Even the squared shaped $30 \times 30 \mu\text{m}^2$ JJ had an almost flat $I_c(H_x)$ pattern. This indicates some magnetic crystallographic anisotropy along the y-axis, probably caused by magnetron sputter deposition. Small deviations of $I_c(0,0)$ for $I_c(H_x,0)$ and $I_c(0,H_y)$ measurements can be related to variations of magnetic configuration by the unshielded sample handling at 300 K. A considerable spread of maximum I_c (Fig. 3) can be already seen for JJs with the same geometry, which is even increased by considering the maximum j_c for different geometries. Simulations (Fig. 2) show that already a moderate magnetization \vec{M} ($\alpha < 0.1$ T/m) yields very different maximum I_c 's of $I_c(H_x)$ and $I_c(H_y)$. A sample to sample variation of direction and amplitude of \vec{M} explains the data spread of Fig. 3. Obviously, this leads to very large variations in the $I_c(d_F)$ dependence.

In literature, the $I_c(H)$ pattern of SFS/SIFS JJs with *comparable* strong magnets were either shown for samples with thin d_F (Ref. 18) or had deviations from the ideal $|\sin(H)/H|$ form. For example, the maximum I_c in Ref. 19 [Fig. 5 (inset)] is too small compared to the first side maxima. These samples were small in area ($\leq 1 \mu\text{m}^2$), and the F-layer could have been in single domain state. As I_c varied smoothly with H , either \vec{M} rotated softly, or a multidomain structure with averaged $2d$ magnetization existed. For both cases the $2d$ nature of remanent magnetization may have suppressed the maximum I_c determined from $I_c(H)$ pattern—below the real I_c^0 .

In summary, the $I_c(H)$ pattern along both field axes of SIFS JJs with Ni interlayer were measured. Assuming magnetic anisotropy the characteristic features, i.e., shift or absence of central peak, can be qualitatively reproduced by

simulations. As conclusion, the $1d$ $I_c(H)$ pattern in the presence of magnetic anisotropy cannot yield the real I_c^0 . Future experiments on SFS/SIFS JJs should be done by two-axis $I_c(H_x, H_y)$ scan of JJs with well-controlled magnetic interlayer domain configuration. Superconducting spintronic devices such as FSF spin valves and π , $0-\pi$ JJs are promising candidates for future classical and quantum computers. As shown by this letter, control of magnetic anisotropy and magnetic domain configuration is essential for phase-switchable FSF/SFIFS or SFS/SIFS devices.

M.W. thanks D. Sprungmann and A. Bannykh for assistance, and DFG for support (Project No. WE 4359/1-1).

¹A. I. Buzdin, *Rev. Mod. Phys.* **77**, 935 (2005).

²V. V. Ryazanov, V. A. Oboznov, A. Y. Rusanov, A. V. Veretennikov, A. A. Golubov, and J. Aarts, *Phys. Rev. Lett.* **86**, 2427 (2001).

³H. Sellier, C. Baraduc, F. Lefloch, and R. Calemczuk, *Phys. Rev. B* **68**, 054531 (2003).

⁴M. Weides, M. Kemmler, E. Goldobin, D. Koelle, R. Kleiner, H. Kohlstedt, and A. Buzdin, *Appl. Phys. Lett.* **89**, 122511 (2006).

⁵Y. Blum, A. Tsukernik, M. Karpovskii, and A. Palevski, *Phys. Rev. Lett.* **89**, 187004 (2002).

⁶T. Kontos, M. Aprili, J. Lesueur, and X. Grisson, *Phys. Rev. Lett.* **89**, 137007 (2002).

⁷V. A. Oboznov, V. V. Bol'ginov, A. K. Feofanov, V. V. Ryazanov, and A. I. Buzdin, *Phys. Rev. Lett.* **96**, 197003 (2006).

⁸A. Bauer, J. Bentner, M. Aprili, M. L. D. Rocca, M. Reinwald, W. Wegscheider, and C. Strunk, *Phys. Rev. Lett.* **92**, 217001 (2004).

⁹V. V. Ryazanov, V. A. Oboznov, A. V. Veretennikov, and A. Y. Rusanov, *Phys. Rev. B* **65**, 020501 (2001).

¹⁰W. Guichard, M. Aprili, O. Bourgeois, T. Kontos, J. Lesueur, and P. Gandit, *Phys. Rev. Lett.* **90**, 167001 (2003).

¹¹M. Weides, M. Kemmler, H. Kohlstedt, R. Waser, D. Koelle, R. Kleiner, and E. Goldobin, *Phys. Rev. Lett.* **97**, 247001 (2006).

¹²M. Weides, C. Schindler, and H. Kohlstedt, *J. Appl. Phys.* **101**, 063902 (2007).

¹³A. V. Ustinov and V. K. Kaplunenko, *J. Appl. Phys.* **94**, 5405 (2003).

¹⁴T. Kato, A. A. Golubov, and Y. Nakamura, *Phys. Rev. B* **76**, 172502 (2007).

¹⁵R. W. Houghton, M. P. Sarachik, and J. S. Kouvel, *Phys. Rev. Lett.* **25**, 238 (1970).

¹⁶V. Shelukhin, A. Tsukernik, M. Karpovskii, Y. Blum, K. B. Efetov, A. F. Volkov, T. Champel, M. Eschrig, T. Löfwander, G. Schön, and A. Palevski, *Phys. Rev. B* **73**, 174506 (2006).

¹⁷J. W. A. Robinson, S. Piano, G. Burnell, C. Bell, and M. G. Blamire, *Phys. Rev. Lett.* **97**, 177003 (2006).

¹⁸C. Bell, R. Loloee, G. Burnell, and M. G. Blamire, *Phys. Rev. B* **71**, 180501 (2005).

¹⁹J. W. A. Robinson, S. Piano, G. Burnell, C. Bell, and M. G. Blamire, *Phys. Rev. B* **76**, 094522 (2007).

²⁰S. A. Ahern, M. J. C. Martin, and W. Sucksmith, *Proc. R. Soc. London* **248**, 145 (1958).

²¹L. Liebermann, J. Clinton, D. M. Edwards, and J. Mathon, *Phys. Rev. Lett.* **25**, 232 (1970).

²²G. Gubbiotti, G. Carlotti, M. G. Pini, P. Politi, A. Rettori, P. Vavassori, M. Ciria, and R. C. O'Handley, *Phys. Rev. B* **65**, 214420 (2002).

²³C. Monton, F. de la Cruz, and J. Guimpel, *Phys. Rev. B* **77**, 104521 (2008).

²⁴A. G. Joshi, S. A. Kryukov, L. E. D. Long, E. M. Gonzalez, E. Navarro, J. E. Villegas, and J. L. Vicent, *J. Appl. Phys.* **101**, 09G117 (2007).

²⁵S. V. Dubonos, A. K. Geim, K. S. Novoselov, and I. V. Grigorieva, *Phys. Rev. B* **65**, 220513 (2002).

²⁶H. Wu, J. Ni, J. Cai, Z. Cheng, and Y. Sun, *Phys. Rev. B* **76**, 024416 (2007).

²⁷F. J. Jedema, B. J. van Wees, B. H. Hoving, A. T. Filip, and T. M. Klapwijk, *Phys. Rev. B* **60**, 16549 (1999).

²⁸M. Weides, K. Tillmann, and H. Kohlstedt, *Physica C* **437-438**, 349 (2006).

²⁹H. Chen, Y. Du, H. Xu, Y. Liu, and J. C. Schuster, *J. Mater. Sci.* **40**, 6019 (2005).